2-2024

Do changes in the real exchange rate affect the trade balance? Evidence from European countries

Jesus Felipe
De La Salle University, Manila, jesus.felipe@dlsu.edu.ph

Jose Antonio Perez-Montiel
jose.perez@uib.es

Öguzhan Ozcelebi
ogozc@istanbul.edu.tr

De La Salle University
AKI
Angelo King Institute
for Economic and Business Studies

DLSU-AKI Working Paper Series
2024-02-091

Do changes in the real exchange rate affect the trade balance? Evidence from European countries

By:

Jesus Felipe
De La Salle University, Manila, Philippines

José A. Pérez-Montiel
University of the Balearic Islands, Spain

Öguzhan Ozcelebi
Istanbul University, Turkey

February 2024

Do changes in the real exchange rate affect the trade balance?

Evidence from European countries

Jesus Felipe (*)

José A. Pérez-Montiel (**)

Öguzhan Ozcelebi (***)

Abstract: We use five time and frequency domain causality tests to study whether unit labor costs-based real exchange rate depreciations / appreciations caused improvements / deteriorations in the trade balances of ten Eurozone economies, and thus contributed to closing trade imbalances, during 1995-2019. The methods we use deal with the inherent nonlinearity, and structural shifts in the time series. They also take into account asymmetry and regime changes. The non-parametric approach avoids the possible bias associated to the identification strategy. Test results indicate that there is no evidence of such a causal relationship.

Keywords: causality tests, effective exchange rate, Europe, unit labor costs

JEL Classification: C14; C32; F16; J31

(*) De La Salle University, Manila, Philippines (jesus.felipe@dlsu.edu.ph); (**) José A. Pérez-Montiel, University of the Balearic Islands, Spain (jose.perez@uib.es); (***) Öguzhan Ozcelebi, Istanbul University, Turkey (ogozc@istanbul.edu.tr). We are grateful to the participants at research seminars at Sant'Anna Scuola Universitaria Superiore Pisa and at the International Astril Conference. The usual disclaimer applies.

1. Introduction

Have real exchange rate shifts contributed to closing (increasing) trade imbalances in the European Union? A widely accepted explanation of the increasing trade imbalances in the Eurozone before 2008 focuses on the functioning of the Economic and Monetary Union (EMU). This explanation argues that the creation of the EMU reduced the risk premia of the European peripheral economies, which led to a consumption and investment boom and, thus, to higher inflation and a loss of competitiveness (via higher unit labor costs) in these countries (Allsop and Vines, 2010; Krugman, 2012; Belke and Dreger 2013; El-Shagi et al. 2016).

Following the global financial crisis of 2008-09, "peripheral" Euro countries (Greece, Ireland, Italy, Spain) were asked (until the Covid-19 crisis) to lower their real wage rates and to increase productivity to reduce their unit labor costs. This was referred to as the *internal depreciation* mechanism.[1] "Core" Euro countries (Finland, France, Germany, Luxemburg, Netherlands, Belgium), on the other hand, were asked to increase their real wage rates and implement policies to increase domestic demand, which would lead to an increase in their unit labor costs. The European Commission supported this strategy to overcome the crisis: "internal devaluation is a set of policies aimed at reducing domestic prices (to regain competitiveness) either by affecting relative export-import prices or by lowering domestic production costs and thus by yielding a real exchange rate depreciation" (European Commission 2011: 22). This economic policy recommendation rests on the idea that real exchange rate adjustments affect the trade balance of the Eurozone economies.

The years after the 2008-09 crisis saw a marked improvement in the trade balances of the Mediterranean economies (Figure 1). According to Hein et al. (2021) and Kohler & Stockhammer (2022), wage restraint and austerity policies contributed to improving the trade balance through the collapse of domestic demand and imports. Figure 1 shows that net exports of Europe's peripheral countries gradually deteriorated right after the start of the second phase of the monetary integration in 1994. Core countries, on the other hand, maintained or increased their trade surpluses. After the 2008-09 crisis, however, the trade deficits of the peripheral countries declined, while the surpluses of some core countries became smaller. This may suggest that internal depreciations led to reductions in the trade imbalances of the European Union.

[1] Given that the members of the Eurozone cannot modify the nominal exchange rates, real exchange rate changes have to result from changes in domestic prices or in production costs.

Figure 1. Net exports as percentage of GDP (1995-2019)

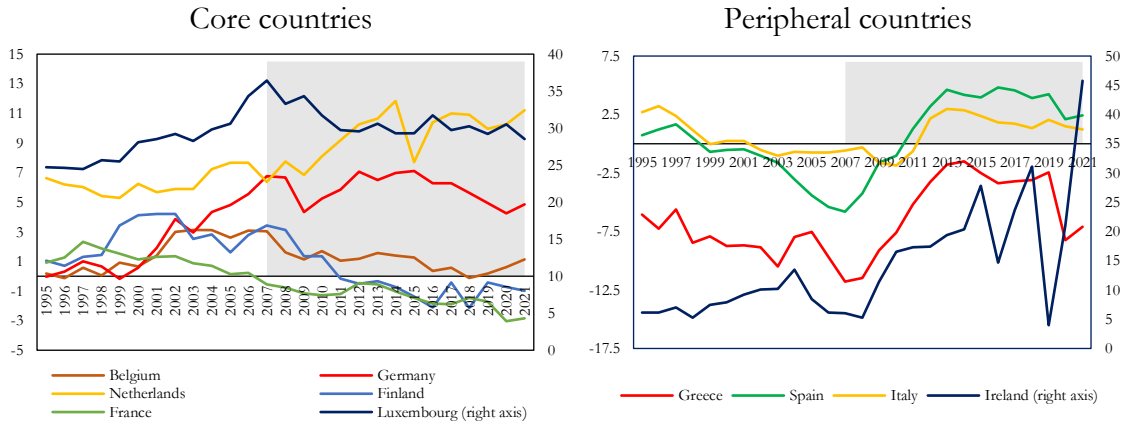

Source: Authors based on Eurostat data.
Note: vertical axis is "Net exports as % of GDP", calculated as: ((exports-imports)/GDP)*100

This paper explores whether internal depreciations corrected trade imbalances in the eurozone. We shed light on this question by analyzing the dynamic causal relationship between the real effective exchange rate based on unit labor costs (q_t) and the trade balance (tb_t). More precisely, we study if negative (positive) changes in q_t caused negative (positive) changes in tb_t in ten Euro Zone economies during 1995-2019.

The relationship between q_t and tb_t has been studied empirically within the approach of Goldstein and Khan (1985). This approach defines the domestic trade balance (tb) as a function of domestic and foreign real income (Y and Y^*, respectively) and the real exchange rate (q):

$$tb = f(Y, Y^*, q). \tag{1}$$

where $\frac{\partial tb}{\partial Y} > 0$, $\frac{\partial tb}{\partial Y^*} < 0$, $\frac{\partial tb}{\partial q} \gtrless 0$, with tb defined as the ratio imports to exports. The sign of $\frac{\partial tb}{\partial q}$ is indeterminate and depends on the price elasticities of exports (ψ) and imports (η). The Marshall-Lerner condition states that the trade balance will improve if the absolute value of the sum of the price elasticities of exports and imports is greater than one; that is $(\frac{\partial tb}{\partial q}\frac{q}{tb}) > 0$ if $|\psi + \eta| > 1$. Following the seminal contribution of Rose and Yellen (1989), a strand of the empirical literature obtains the elasticity of the trade balance with respect to the real exchange rate by directly estimating (1) as:

$$lntb_t = \alpha + \beta_1 lnY_t^* + \beta_2 lnY_t + \beta_3 lnq_t \tag{2}$$

If $\beta_3 > 0$ and statistically significant, it is concluded that a depreciation (appreciation) improves (worsens) the trade balance in the long run. Some applications allow for a dynamic response of the different explanatory variables, so that the short-term elasticity of the exchange rate can be smaller than the long-term elasticity, thereby producing a J-curve effect (Magee 1973). However, the effects of changes in real exchange rate on the trade balances

of the Euro zone are empirically inconclusive. See Bahmani et al. (2013) for a review of the literature, and Bahmani-Oskooee and Nouira (2021a) for a recent empirical application.

The main novelty of this paper with respect to the existing literature is that it applies a battery of non-parametric causality tests in the time and frequency domains. The tests are: the parametric causality-in-quantile test of Troster (2018); the nonparametric causality-in-quantile test of Balcilar et al. (2017); the rolling-window Granger-causality test of Hacker and Hatemi-J (2012); the partial wavelet coherence (PWC) approach; and the Wavelet Quantile Correlation (WQC) technique of Li et al. (2015). The main advantages of the causality tests that we apply to equation (2) is that they overcome many of the shortcomings of the traditional Granger causality tests used in the exchange rate-trade balance literature (Bahmani-Oskooee and Nouira, 2021b). They deal with the inherent nonlinearity and structural shifts in the time series, consider asymmetry and regime changes, and the non-parametric approach avoids the possible bias associated to the identification strategy.

The remainder of the paper is structured as follows. Section 2 describes the variables and the empirical approach. Section 3 describes our econometric methodology. Section 4 discusses the empirical results. Finally, Section 5 concludes. The Appendix provides details of the tests we use.

2. Data and empirical approach

Following the seminal contribution of Rose and Yellen (1989) and the literature afterwards, we consider that the trade balance (tb_t) is a function of the real exchange rate (q_t), domestic economic activity (Y_t) and global economic activity (Y_t^*).

In this paper, we focus on the relationship between tb_t and q_t in ten European economies: Spain, Ireland, Greece, Belgium, Luxemburg, Netherlands, France, Germany, Italy, and Finland. The trade balance (tb_t) is the ratio of imports (M_t) to exports (X_t) of goods and services. Since $tb_t = M_t / X_t$, a positive (negative) change in tb_t indicates a deterioration (improvement) of the trade balance.

The real exchange rate (q_t) is the real effective exchange rate (REER), based on unit labor costs (ULC), with respect to the 37 main industrial countries. It is constructed and provided by Eurostat, and its unit is the Index 2010=100 (see Mazzocchi and Tamborini, 2021). The real effective exchange rate for each country i is defined as:

$$q_{it} = \sum_j \omega_{ijt}\, e_{ijt} \frac{ULC_{it}}{ULC_{jt}} \tag{3}$$

where j denotes the trading partners, ω_{ij} are the bilateral trade weights in period t, e_{ijt} are the bilateral nominal exchange rates, and ULC_{it}/ULC_{jt} are the bilateral relative unit labor costs (or relative efficiency wages), defined as the ratio of labor costs (nominal wage rate) to labor productivity:

$$ULC_t = \frac{w_t}{Y_t/E_t} \tag{4}$$

where w_t is the average nominal wage rate; Y_t is real gross domestic product at market prices (in millions, chain-linked volumes, base year 2010); and E_t indicates total employment (all industries, in number of persons). It includes both employees and the self-employed. Because of how q_{it} is constructed, a positive (negative) change in it denotes an appreciation (depreciation) of the real effective exchange rate of country i. Thus, we expect a positive correlation between q and tb.

Figure 2 shows the trade balance and the real effective exchange rate of the ten countries under study. We can appreciate a progressive increase in the trade deficits of Greece and Italy since 1995. Spain started experiencing a progressive increase in its deficit after the euro was launched in 1999. This increasing deficit lasted until the Great Recession. From this moment onwards, these three countries reduced their trade deficits, and Spain and Italy attained a surplus. The situation of the core European countries is different. They experimented a progressive improvement in their trade balances since 1995, with a sole interruption in 2009.

As stated above, we control for domestic and global economic activity. Domestic economic activity (Y_t) is proxied by the country's gross domestic product (chain linked volumes 2010, in million euros). Global economic activity (Y_t^*) is proxied by the updated index of global real economic activity in industrial commodity markets of Kilian (2019).[2] This is a business-cycle index expressed in percent deviation from the trend. All data are taken in logarithms; accordingly, the first-differenced series express growth rates. The data for tb_t, q_t, and Y_t are from the Eurostat database, while the data for Y_t^* are from the Federal Reserve Bank of Dallas database.

[2] It is a proxy for the volume of shipping in global industrial commodity markets. It is derived from a panel of dollar-denominated global bulk dry cargo shipping rates. The advantages of this index compared with the global real GDP or the global industrial production index are discussed in Killian and Zhou (2018).

Figure 2. Real effective exchange rate (q_t) and trade balance (tb_t)

Source: Authors' elaboration based on Eurostat quarterly data.

Notes: (i) Trade balance (tb_t) is the ratio of imports (M_t) to exports (X_t) of goods and services ($tb_t = M_t / X_t$). Exports and imports are measured in Chain linked volumes, index 2010=100 (Unadjusted data, i.e., neither seasonally adjusted nor calendar adjusted data); (ii) Real effective exchange rate, Index 2010=100.

Table 1 shows the descriptive statistics (mean, maximum and minimum values, standard deviation, skewness, and kurtosis) of the series. It also shows the Jarque-Bera (JB) normality test, and unit root tests of the variables in log-first differences, i.e., growth rates (denoted Δ). The ADF and PP unit root tests indicate that both Δq and Δtb are stationary. The skewness and kurtosis tests indicate that the series are not normally distributed; and the Jarque-Bera test for tb_t rejects the null hypothesis of normality at the 5% significance level. This suggests the appropriateness of using nonlinear models that are robust to non-normal skewness in estimation.

Table 1. Descriptive statistics and unit root tests

Variable: q_t	Belgium	Netherlands	Finland	Luxemburg	Ireland	Spain	Greece	Italy	Germany	France
Mean	0,00	0,00	0,00	0,00	-0,00	0,00	0,00	0,00	-0,00	0,00
Median	0,00	0,00	0,00	0,00	0,00	0,00	0,00	0,00	0,00	0,00
Maximum	0,01	0,01	0,02	0,01	0,02	0,01	0,02	0,03	0,01	0,01
Minimum	-0,01	-0,01	-0,02	-0,01	-0,05	-0,01	-0,02	-0,03	-0,01	-0,01
Std. Dev.	0,00	0,00	0,00	0,00	0,01	0,00	0,007	0,01	0,01	0,01
Skewness	-0,06	-0,21	-0,21	-0,02	-1,04	-0,07	-0,12	0,29	-0,08	-0,07
Kurtosis	3,05	3,17	3,42	3,57	6,51	2,70	3,22	6,75	2,87	2,64
Jarque-Bera	0,08	0,8	1,47	1,35	68,91	0,45	0,43	59,54	0,17	0,59
	(0,96)	(0,65)	(0,48)	(0,51)	(0,00)	(0,71)	(0,80)	(0,00)	(0,92)	(0,74)
No. Obs.	99	99	99	99	99	99	99	99	99	99
ADF	-4,21	-3,23	-3,51	-3,78	-3,77	-2,18	-1,54	-8,20	-7,02	-6,98
	(0,00)	(0,02)	(0,00)	(0,00)	(0,00)	(0,21)	(0,50)	(0,00)	(0,00)	(0,00)
PP	-71,63	-28,33	-28,76	-24,92	-13,03	-32,28	-11,81	-8,74	-7,24	-7,10
	(0,00)	(0,00)	(0,00)	(0,00)	(0,00)	(0,00)	(0,00)	(0,00)	(0,00)	(0,00)

Variable: tb_t	Belgium	Netherlands	Finland	Luxemburg	Ireland	Spain	Greece	Italy	Germany	France
Mean	0,00	0,00	0,00	0,00	0,00	-0,00	-0,00	0,00	0,00	0,00
Median	0,00	-0,00	0,00	0,00	-0,00	-0,01	-0,03	0,00	0,00	0,00
Maximum	0,02	0,13	0,09	0,04	0,20	0,07	0,25	0,05	0,03	0,02
Minimum	-0,02	-0,09	-0,07	-0,04	-0,24	-0,05	-0,17	-0,04	-0,03	-0,02
Std. Dev.	0,01	0,02	0,02	0,02	0,06	0,03	0,13	0,02	0,01	0,01

Skewness	-0,15	1,56	0,48	-0,29	-0,05	0,42	0,43	-0,09	-0,14	0,25
Kurtosis	4,27	20,68	5,15	4,64	9,98	2,05	1,69	1,93	2,57	3,11
Jarque-Bera	7,00	1328,84	22,93	12,40	201,16	6,68	10,08	4,81	1,10	1,06
	(0,03)	(0,00)	(0,00)	(0,00)	(0,00)	(0,08)	(0,01)	(0,09)	(0,58)	(0,59)
No. Obs.	99	99	99	99	99	99	99	99	99	99
ADF	-9,03	-9,70	-11,69	-10,62	-5,93	-2,34	-5,50	-3,19	-4,54	-7,77
	(0,00)	(0,00)	(0,00)	(0,00)	(0,00)	(0,15)	(0,00)	(0,02)	(0,00)	(0,00)
PP	-24,30	-36,85	-31,61	-76,41	-41,19	-13,34	-17,89	-15,15	-16,76	-15,29
	(0,00)	(0,00)	(0,00)	(0,00)	(0,00)	(0,00	(0,00)	(0,00)	(0,00)	(0,00)

Source: Authors; ADF: Augmented Dickey-Fuller; PP: Phillips-Perron.

Note: the ADF and PP tests refer to the growth rates, i.e., Δq and Δtb.

3. Econometric Methodology

The first step is to test whether the relationship between Δtb_t and Δq_t is linear against the alternative of nonlinear. We use the BDS test of Brock et al. (1996). The results of the test (Table 2) reject the null hypothesis and indicate that the relationship between the two variables is nonlinear. These results suggest the necessity of applying nonlinear tests to study the nexus between Δq_t and Δtb_t. It is in line with the findings of Nogueira and León-Ledesma (2011), who suggest that exchange rates pass-through into consumer prices are nonlinear. This result implies that the relationship between the exchange rate and the trade balance must be analyzed by means of nonlinear econometrics.

Table 2. BDS test results

Dimension	Belgium	Netherlands	Finland	Luxemburg	Ireland	Spain	Greece	France	Germany	Italy
2	0,00	0,00	0,00	0,00	0,00	0,00	0,00	0,00	0,00	0,00
3	0,00	0,00	0,00	0,00	0,00	0,00	0,00	0,00	0,00	0,00
4	0,00	0,00	0,00	0,00	0,00	0,00	0,00	0,00	0,00	0,00
5	0,00	0,00	0,00	0,00	0,00	0,00	0,00	0,00	0,00	0,00
6	0,00	0,00	0,00	0,00	0,00	0,00	0,00	0,00	0,00	0,00

Dimension	Belgium	Netherlands	Finland	Luxemburg	Ireland	Spain	Greece	France	Germany	Italy
2	0,00	0,03	0,00	0,00	0,00	0,00	0,00	0,00	0,89	0,13
3	0,00	0,00	0,00	0,00	0,00	0,00	0,45	0,00	0,94	0,00
4	0,00	0,00	0,00	0,00	0,00	0,00	0,54	0,00	0,35	0,00
5	0,00	0,00	0,00	0,00	0,00	0,00	0,00	0,00	0,01	0,00
6	0,00	0,00	0,00	0,00	0,00	0,00	0,00	0,01	0,00	0,00

Source: Authors.

3.1. Time-domain causality tests

Standard Granger-causality tests (Granger, 1969) assume that the parameters of the vector autoregressive (VAR) model are constant over time. However, time series data usually exhibit structural changes that the standard Granger-causality tests do not capture. Researches can identify and incorporate structural changes into the estimation by splitting the sample and by adding dummy variables, but these procedures introduce pretest bias. In what follows, we outline the time series techniques that we use to study the nexus between Δtb_t and Δq_t within the time-domain approach. In order to overcome the possible parameter non-constancy and avoid pretest bias, we adopt both quantile Granger-causality and rolling-window Granger-causality approaches. The Appendix provides details of the tests.

We use two Quantile Granger-causality tests. Since Granger-causality tests in mean overlook the possible relationships in the conditional tails of the distribution, we test for Granger causality across different quantiles of the conditional distribution. Quantile Granger causality tests examine if the causal relationship between Δq_t and Δtb_t is asymmetric across the distribution. In order to consider the role of regimes in the dependent variable, we first use the parametric approach of Troster (2018) to test for Granger-noncausality in conditional quantiles. It allows to identify the pattern of causality and provides a sufficient condition for Granger causality. Denoting $Q_\tau(W_{t-1}) \equiv Q_\tau(\Delta tb_t|W_{t-1})$ and $Q_\tau(TB_{t-1}) \equiv Q_\tau(\Delta tb_t|TB_{t-1})$, the null hypothesis of no Granger-causality from Δq_t to Δtb_t in the τ-th quantile is:

$$H_0 = P\{F_{\Delta tb_t|W_{t-1}}\{Q_\tau(TB_{t-1})|W_{t-1}\} = \tau\} = 1, \tag{5}$$

while the alternative that Δq_t Granger-causes Δtb_t in the τ-th quantile is:

$$H_1 = P\{F_{\Delta tb_t|W_{t-1}}\{Q_\tau(TB_{t-1})|W_{t-1}\} = \tau\} < 1. \tag{6}$$

Second, we apply the nonparametric causality-in-quantile test of Balcilar et al. (2017). To the best of our knowledge, this is the first article in the exchange rate-trade balance nexus literature that uses a nonparametric Granger causality method. The non-parametric test of Balcilar et al. (2017) is a model-free method, robust to the misspecification of the quantile regression. The method also accounts for the existence of possible outliers and structural breaks. Based on Jeong et al. (2012), Balcilar et al. (2017) overcome the problem between the difference between causality in mean and causality in variance. The hypothesis of quantile Granger-causality from Δq_t to Δtb_t in higher-order moments is specified as:

$$H_0 = P\left\{F_{\Delta tb_t^K|W_{t-1}}\{Q_\tau(TB_{t-1})|W_{t-1}\} = \tau\right\} = 1 \; for \; k = 1, 2, \dots, K, \tag{7}$$

and the alternative as:

$$H_1 = P\left\{F_{\Delta tb_t^K|W_{t-1}}\{Q_\tau(TB_{t-1})|W_{t-1}\} = \tau\right\} < 1 \; for \; k = 1, 2, \dots, K. \tag{8}$$

We also use a rolling-window Granger-causality test, specifically the Hacker and Hatemi-J (2012) time-varying approach. This test relies on fixed-size subsamples rolling sequentially from the beginning to the end of the sample by adding one observation from ahead and dropping one from behind. The test is applied to each subsample, instead of estimating a singly causality test for the entire sample. Possible changes in the causal linkages between the variables can be intuitively identified by calculating the bootstrap *p*-values of observed LR statistics rolling through the subsamples. The test is based on the lag-augmented VAR (LA-VAR) model specification of Toda and Yamamoto (2000):

$$Y = DZ + \delta \tag{9}$$

In equation (9), $Y := (y_1, y_2, \ldots, y_T)$ refers to an $(n \times T)$ matrix in which n is the number of variables and T is the sample size. In this framework, $D := (\alpha, A_1, A_2, \ldots, A_k)$ is an $(n \times (1 + (k + d_{\max}))$ matrix and $Z := (Z_0, Z_1, \ldots, Z_{T-1})$ denotes a $((1 + n(k + d_{\max})) \times T)$ matrix. Thus, a matrix can be written as:

$$Z_t := \begin{bmatrix} 1 \\ y_t \\ y_{t-1} \\ . \\ . \\ y_{t-k+1} \end{bmatrix},$$

and $\delta := (u_1, u_2, \ldots, u_T)$ represents a $(n \times T)$ matrix. Equation (A16) constitutes a framework test for the null of no causality. The null hypothesis of Granger-noncausality is:

$$H_0 : C\beta = 0 \tag{10}$$

and can be tested through the following Wald statistic:

$$\text{Wald} = (C\beta)'[C((Z'Z)^{-1} \otimes S_u)C']^{-1}(C\beta) \sim X_p^2 \tag{11}$$

where $\beta = vec(D)$, vec is the column-stacking operator, $\otimes$ is the Kronecker product, C is a (p × n)(1 + p × n) indicator matrix with ones and zeros, and S_u is the variance-covariance matrix of the unrestricted VAR model. Additionally, we incorporate the role of asymmetry in the rolling-window Granger causality framework. This is important because it allows us to separately study if depreciations (appreciations) Granger-cause improvements (deteriorations) in the trade balance.

3.2. Combined Time- and frequency-domain causality tests

We also investigate how Δq_t and Δtb_t relate to each other at different frequencies, and how this relationship changes over time. We conduct two tests. The Appendix provides details of the tests.

We start the time- and frequency-domain analyses by applying the partial wavelet coherence (PWC) approach to capture the co-movement of Δq_t and Δtb_t. This is a non-

parametric method that allows the decomposition of a time series into the bi-dimensional time–frequency sphere. As suggested by Granger (1969), the strength and direction of causal relationships among variables may vary over different frequencies. Fourier transformations (FT) can be used to focus on the frequency domain of the variables. However, FT do not provide information on how the frequency components of the time series change over time. Therefore, time information is lost. This means that Fourier analysis is not appropriate to analyze time-varying relationships between economic variables. Wavelet analysis overcomes this problem by incorporating both the frequency and the time-varying features of a series. The advantage of wavelet analysis over FT is that it considers time domain as well as frequency domain. For these reasons, we use wavelet analysis. This permits the analysis of the long- and the short-run causal linkages between Δq_t and Δtb_t across different time scales.

The Wavelet Coherence (WC) of two series $\Delta q = \{\Delta q_{\mathrm{n}}\}$ and $\Delta tb = \{\Delta tb_{\mathrm{n}}\}$ is the localized correlation coefficient among these variables in the time-frequency domain. We calculate the WC as the squared absolute value of the smoothed cross wavelet spectrum normalized by the product of the smoothed individual wavelet partial spectrum of each variable:

$$R^2(u,s) = \frac{\left|S\left(s^{-1}W_{\Delta q \Delta tb}(u,s)\right)\right|^2}{S\left(s^{-1}\left|W_{\Delta q}(u,s)\right|^2\right)S(s^{-1}|W_{\Delta tb}(u,s)|^2)} \tag{12}$$

where for each signal Δq and Δtb, the individual wavelet spectra is $W_n^{\Delta q}(s)$ and $W_n^{\Delta tb}(s)$. The Cross-Wavelet between two signals is expressed as $CWS_n^{\Delta q \Delta tb}(s) = W_n^{\Delta q}(s)W_n^{\Delta tb^*}(s)$, where $W_n^{\Delta tb^*}$is the complex conjugate of $W_n^{\Delta tb}(s)$. The CWP is thus defined as $\left|W_n^{\Delta q \Delta tb}\right|$. The Wavelet Coherence (WC) of two series $\Delta q = \{\Delta q_{\mathrm{n}}\}$ and $\Delta tb = \{\Delta tb_{\mathrm{n}}\}$ is the localized correlation coefficient among these variables in the time-frequency domain. We calculate WC as the squared absolute value of the smoothed CWS normalized by the product of the smoothed individual WPS of each variable.

Second, we use the newly proposed Wavelet Quantile Correlation (WQC) technique to consider the role of regimes and the frequency domain. The WQC procedure is a notable extension of the quantile correlation estimator inspired by Percival and Walden (2000) and Li et al. (2015). The WQC estimator allows information identification over different quantiles and time horizons. The model also considers tail and structure dependence across differing time dimensions. Likewise, the WQC procedure allows the study of the dynamic dependence structure over varying time scales. Additionally, the procedure adequately captures the potentiality of asymmetric association among the series and over their distributions. The quantile correlation method is implemented by Kumar and Padakandla (2022) by means of a maximal overlapping discrete wavelet transform to decompose Δq_t and Δtb_t. Pairs of Δq_t and Δtb_t are decomposed at the j_{th} level, and quantile correlation techniques are applied to get the wavelet quantile correlation for each level j. The wavelet quantile correlation is:

$$WQC_t(\Delta tb, \Delta q) = \frac{QC_t(d_j[\Delta tb], d_j[\Delta q])}{\sqrt{var(\theta_\tau(d_j[\Delta tb] - Q_{\tau,d_j[\Delta tb]}))var(d_j[\Delta q])}} \quad (13)$$

where $Q_{\tau,\Delta q}$ is the τ-th quantile of Δq, and $Q_{\tau,\Delta tb}(\Delta q)$ the τ-th quantile of Δtb conditioning on Δq.

4. Empirical results

This section summarizes our results:

(i) To implement the Granger causality test in quantiles of Troster (2018), we specify nonlinear CAViaR models under the null of no Granger-causality.[3] We compare the root mean squared error (RMSE) of 120 recursive out-of-sample forecasts of the quantiles τ = {0.1, 0.3, 0.5, 0.7, 0.9} of the distribution of Δtb_t. We find that the nonlinear CAViaR models overall outperform linear quantile models. This justifies using these specifications to test for Granger causality in quantiles between Δq_t and Δtb_t. Nevertheless, results do not qualitatively change if we use the linear quantile autoregressive (QAR) models instead of the nonlinear specifications. Figure 3 shows the results, which indicate no evidence of causality from Δq_t to Δtb_t at any quantile of the conditional distribution of Δtb_t. Figure 3 indicates that the estimated subsampling *p*-values do not reject the null hypothesis of Granger non-causality from Δq_t to Δtb_t at any quantile for any country. Therefore, we do not find any evidence of causality from Δq_t to Δtb_t across the whole conditional distribution of Δtb_t.

[3] We used the Matlab code provided by Ahmed et al. (2022).

Figure 3. Nonlinear quantile-causality from Δq_t to Δtb_t (CAViaR models)

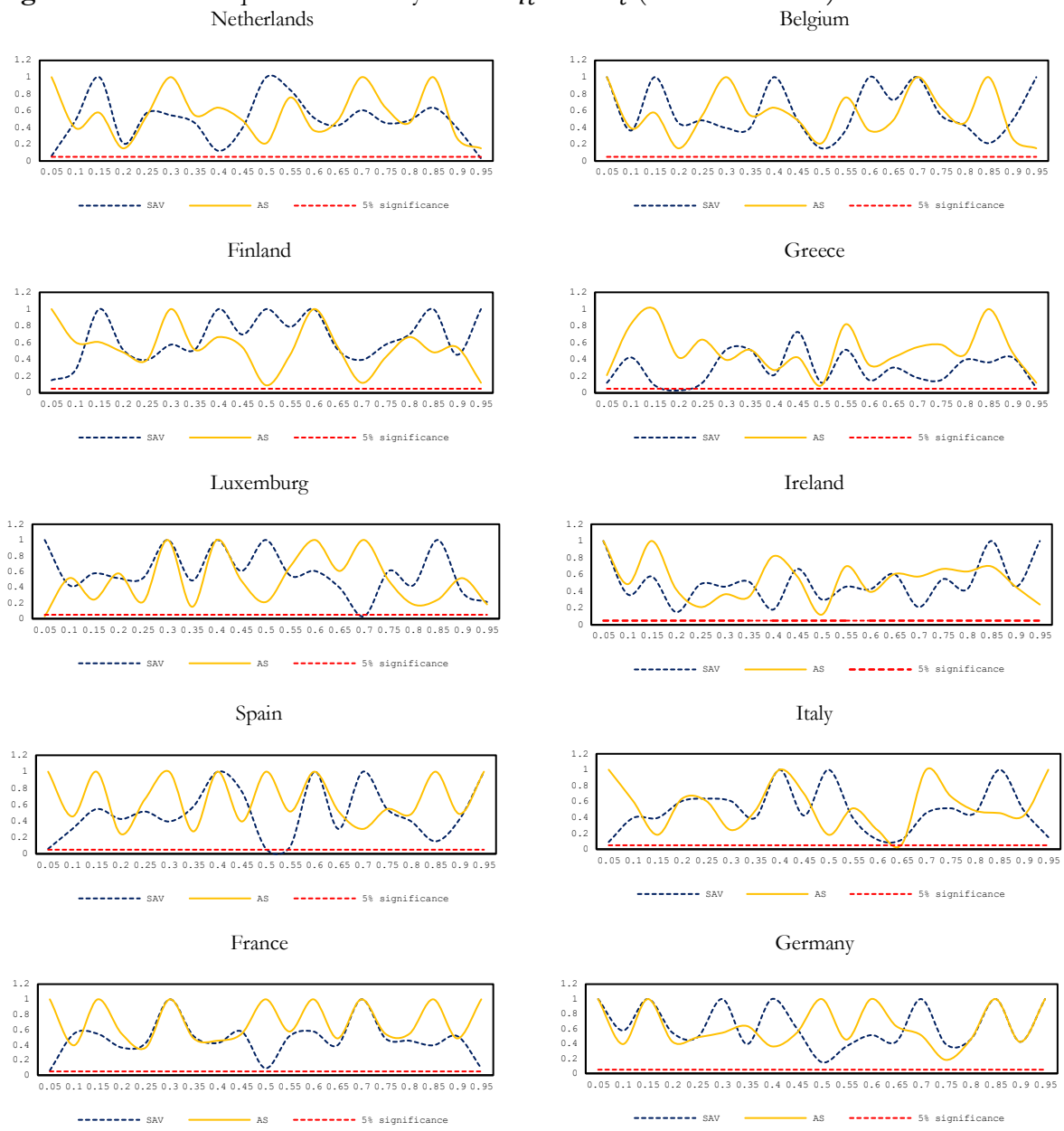

Source: Authors.

Note: This Figure shows the subsampling *p*-values of the CAViar tests for Spain, Ireland, Greece, France and Italy. The red dashed line indicates the 5% significance level p-value. The *p*-values under the red dashed line indicate rejection of the null hypothesis of no Granger causality at the 5% significance level. SAV is the symmetric absolute value model, while AS is the asymmetric slope model.

(ii) Given the lag-dependence of the Granger causality found through the Troster (2018) test, we also applied the model-free Granger-causality in quantiles test of Balcilar et al. (2017).[4] Figures 4 and 5 show the results of the of the Balcilar et al. (2017) non-parametric Granger-causality in quantiles test in mean between Δq_t and Δtb_t. The vertical axis shows the test statistic for each quantile (shown in the horizontal axis). The 5% critical value is 1.96 (red

[4] Professor Balcilar very kindly provided us with the R code to implement this test.

line) and the 10% critical value is 1.64 (dashed line). Lower, middle and higher quantiles (in the horizontal axis), relate to stuck, normal and booming periods/conditions of the exchange rate and the trade balance.

Figure 4 indicates that, except for Spain and Greece, all test statistics are below the critical value of 5% across all quantiles of the conditional distribution of Δtb_t. For Spain, Δq_t Granger-causes Δtb_t over the quantile range of 0.15–0.70. This suggests that changes in q_t cause changes in tb_t in the middle tails of the conditional distribution of Δtb_t, but not in the extreme tails. In other words: Δq_t helps predict Δtb_t in *normal* times, but not in extreme booms of the trade balance such as the one experienced by Spain after the Great Recession. Overall, these results are in line with those of the parametric Granger causality in quantiles test of Troster (2018), suggesting sparse evidence of causality from Δq_t to Δtb_t.

Figure 5 shows no Granger causality running from Δtb_t to Δq_t except for Finland over the range of quantiles [0.25; 0.5], which implies that in this country depreciations are caused by changes in the trade balance.

Figure 4. Balcilar (2017) non-parametric quantile Granger causality from Δq_t to Δtb_t.

Source: Authors

Figure 5. Balcilar (2017) non-parametric quantile Granger causality from Δtb_t to Δq_t

Source: Authors.

(iii) Since we have found evidence of Granger causality from Δq_t to Δtb_t at some quantiles of the conditional distribution of Δtb_t for Spain and Greece, we apply the rolling-window Granger-causality test of Hacker and Hatemi-J (2012) to these two countries.[5] Since the rolling-window Granger causality framework allows for time-varying effects, we can identify the periods in which depreciations (appreciations) have Granger-caused improvements (deteriorations) in the trade balance in Spain and Greece. Figure 6 shows the results of the

[5] We used the Gauss code provided by Yilanci and Kilci (2021).

time-varying bootstrap causality test. The horizontal axis depicts the time-period, while the *p*-values obtained by the test are measured along the vertical axis.

The left hand-side of the Figure shows the results of the Granger causality test running from depreciations (Δq_t^-) to improvements in the trade balance (Δtb_t^-); while the right-hand side shows the results of the Granger causality test from appreciations (Δq_t^+) to deteriorations in the trade balance (Δtb_t^+). We find little empirical support for the argument that real exchange rates predicted trade balances before the Great Recession. Figure 6 indicates that depreciations contributed to the improvement of the trade balance in Spain only at the end of the period under study, in 2019. On the other hand, the predictive power of appreciations on trade balance deteriorations is significant in Greece during 2000-2003. That is, the trade balance of this country deteriorated due to real exchange rate appreciations only between 2000 and 2003. Overall, the results of the time-varying bootstrap Granger causality are in line with the Granger causality in quantiles tests, indicating sparse evidence of causality from exchange rate changes to trade balance changes.

Figure 6. Hacker and Hatemi-J (2012) rolling-window Granger causality.

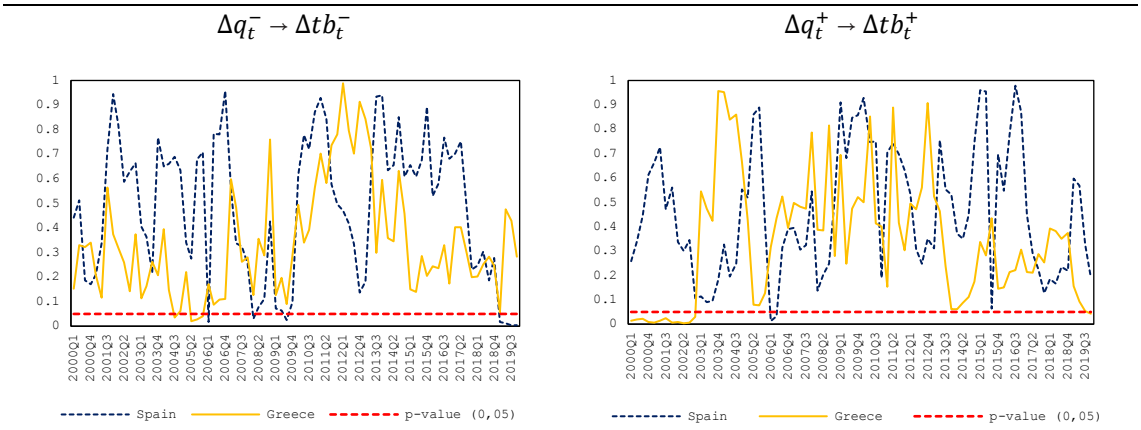

Source: Authors.

(iv) We next test the causal relationship between Δq_t and Δtb_t within the time-frequency domain by means of the partial wavelet coherency (PWC).[6] Compared to the time-domain approach, this method provides a better understanding of the nature of the lead-lag relationship between Δq_t and Δtb_t insofar as it allows to study the frequency components of the time series without losing the time information.

Figure 7 shows the wavelet coherence plots, which provide information about the magnitude of the effect that a shock in one variable has on the other one. We display the mean values for the phase-differences and partial gains corresponding to the two frequency bands considered, namely for cycles of 9∼16 and 22∼28 quarters. We measure the phase-

[6] To construct the wavelet coherence plots, we used the Matlab code from https://grinsted.github.io/wavelet-coherence/.

differences on a circular scale and compute their mean as a circular one. Each wavelet measure is a function of t (time) and s (scale or frequency). The wavelet power and the wavelet coherencies are plotted as 2-dimensional heat-maps, with colors ranging from blue (low power/small coherency) to yellow (high power/high coherency). The black contours show the 5% significance level of co-movements between Δtb_t and Δq_t, derived from an ARMA (1, 1) model. We measure the time-period along the x-axis and the frequency (scale) along the y-axis. Thus, the plot clearly identifies both frequency bands and time intervals where the series move together.

Figure 7 also shows the relative phasing of the variables by means of phase arrows, which indicate the direction of interdependence and cause–effect relationships. Arrows pointing to the left indicate that the variables are in phase (positive correlation), while arrows pointing to the right indicate that the variables are in antiphase (negative correlation). If the arrows point to the right and up, then the phase-difference lies between 0 and $\pi/2$, and both series move in the phase but the former variable (Δtb_t) leads the latter (Δq_t). If the arrows point to the right and down, the phase-difference lies between $-\pi/2$ and 0, and then Δq_t leads Δtb_t. If the arrows point to the left and up, the partial phase-difference lies within the range $(\pi/2; \pi)$, which means that Δq_t leads Δtb_t. Finally, if the arrows point to the left and down, the phase-difference lies within $(-\pi; -\pi/2)$ and Δtb_t leads Δq_t. Therefore, the condition for same-sign causality from Δq_t to Δtb_t is that the phase-difference between Δtb_t and Δq_t in the regions of high partial coherence lie between $\pi/2$ and π, i.e., arrows point to the left and up.

Figure 7. Wavelet coherence plots.

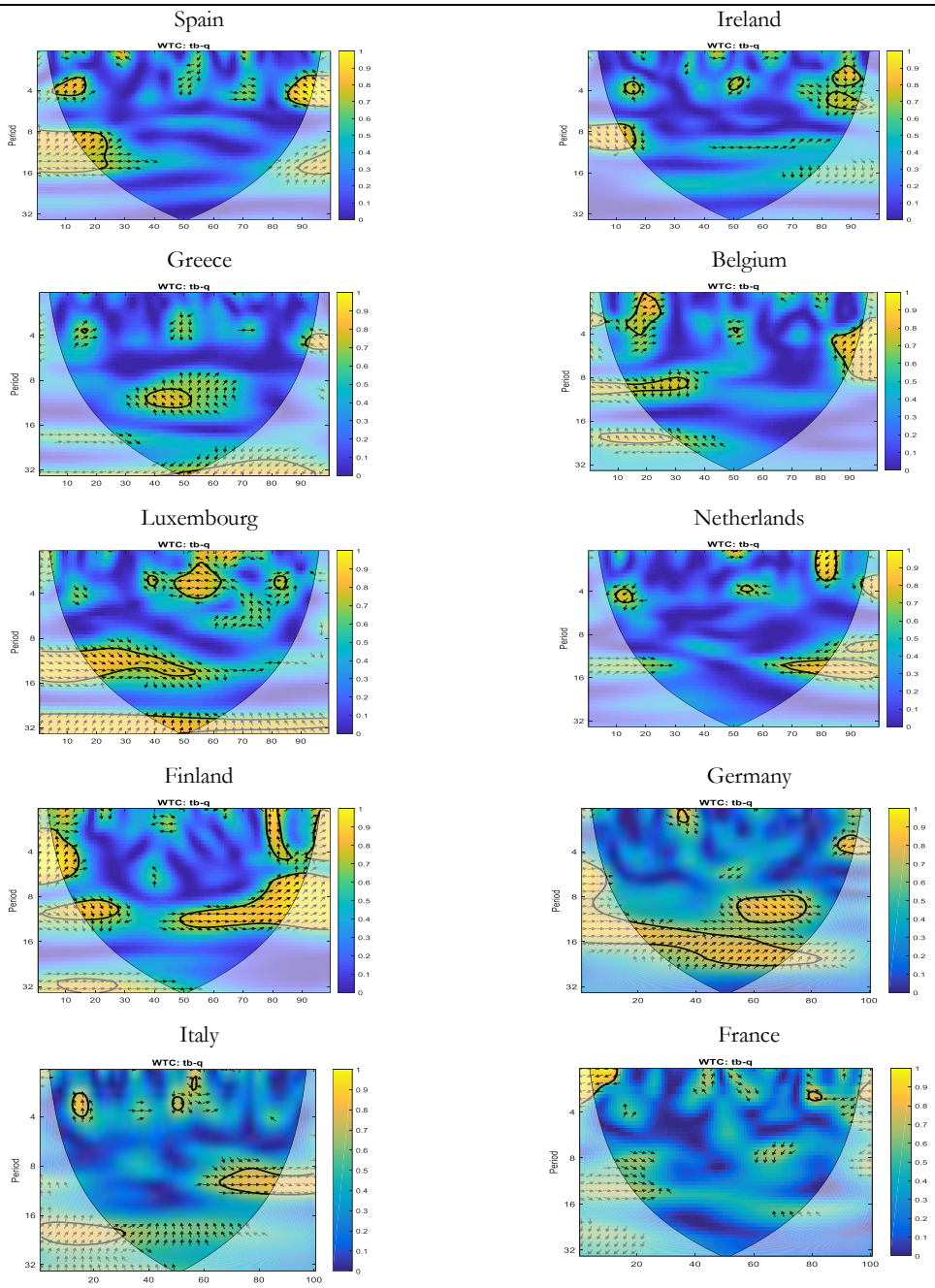

Source: Authors.

Note: Phase arrows indicate the direction of co-movement between tb and q. The thick black contour lines indicate the 5% significance intervals estimated from Monte Carlo simulations with phase randomized surrogate series. The cone of influence, which marks the region affected by edge effects, is shown with a lighter shade black line. The color legend for spectrum power ranges from Blue (low power) to yellow (medium power) and red (high power). Y-axis measures frequency (scale) and X-axis represents the time period.

First, the multiple directions of the arrows indicate that the interdependence between Δq_t and Δtb_t is not homogeneous across different times and scales. Second, we see that for Spain, Δq_t leads Δtb_t for the time scale of 3–5-quarter frequency band for 2016-2019; and for Greece, Δq_t leads Δtb_t for the time scale of 10–14-quarter frequency band for 2000-

2007. For the rest of the countries, however, there is no evidence of a same-sign relationship between changes in exchange rate and trade balance. This result is in line with the results of the time-domain analysis and conflicts with the conventional wisdom of an overall significant exchange rate-trade balance causal nexus in Europe.

(v) Finally, we applied the newly proposed Wavelet Quantile Correlation (WQC) technique of Li et al. (2015).[7] The WQC procedure is a notable extension of the quantile correlation estimator inspired by Percival and Walden (2000). Figure 8 shows the results. We extract information at the scales of 2-4 quarters, 4–8 quarters (short run), 8-16 quarters (medium run), and 16–32 quarters (long run). The deep black color boxes denote a negative quantile correlation between the variables. Conversely, the highly yellow color boxes represent a positive association, denoting the exchange rate's same-sign effects on the trade balance.

In Figure 8 we can see that the quantile correlation between Δq_t and Δtb_t reveals varying effects of the former on the latter across the quantile distributions of tb. Above all, we observe positive correlation coefficients in all countries, but they are not sufficiently high to conclude that the variables are dynamically connected. The exception is Germany, which presents a relevant positive association between Δq_t and Δtb_t at medium quantiles in the long run. For this country, we observe a sort of J-curve relationship (Magee 1973) between Δq_t and Δtb_t, since the former negatively (positively) affects the latter in the short run (long run). On the other hand, at some quantile and time frequencies, we observe that the variables are negatively correlated (despite the coefficient of correlation not being so significant) in the long run for Spain, Ireland, Belgium, Luxemburg, Finland and France. This result might partly align with the theoretical and empirical literature indicating contractionary effects of currency devaluation (Krugman and Taylor 1978; Fukui et al. 2023).

[7] We used the R code provided by Kumar and Padakandla (2022).

Figure 8. Wavelet Quantile Correlation (WQC).

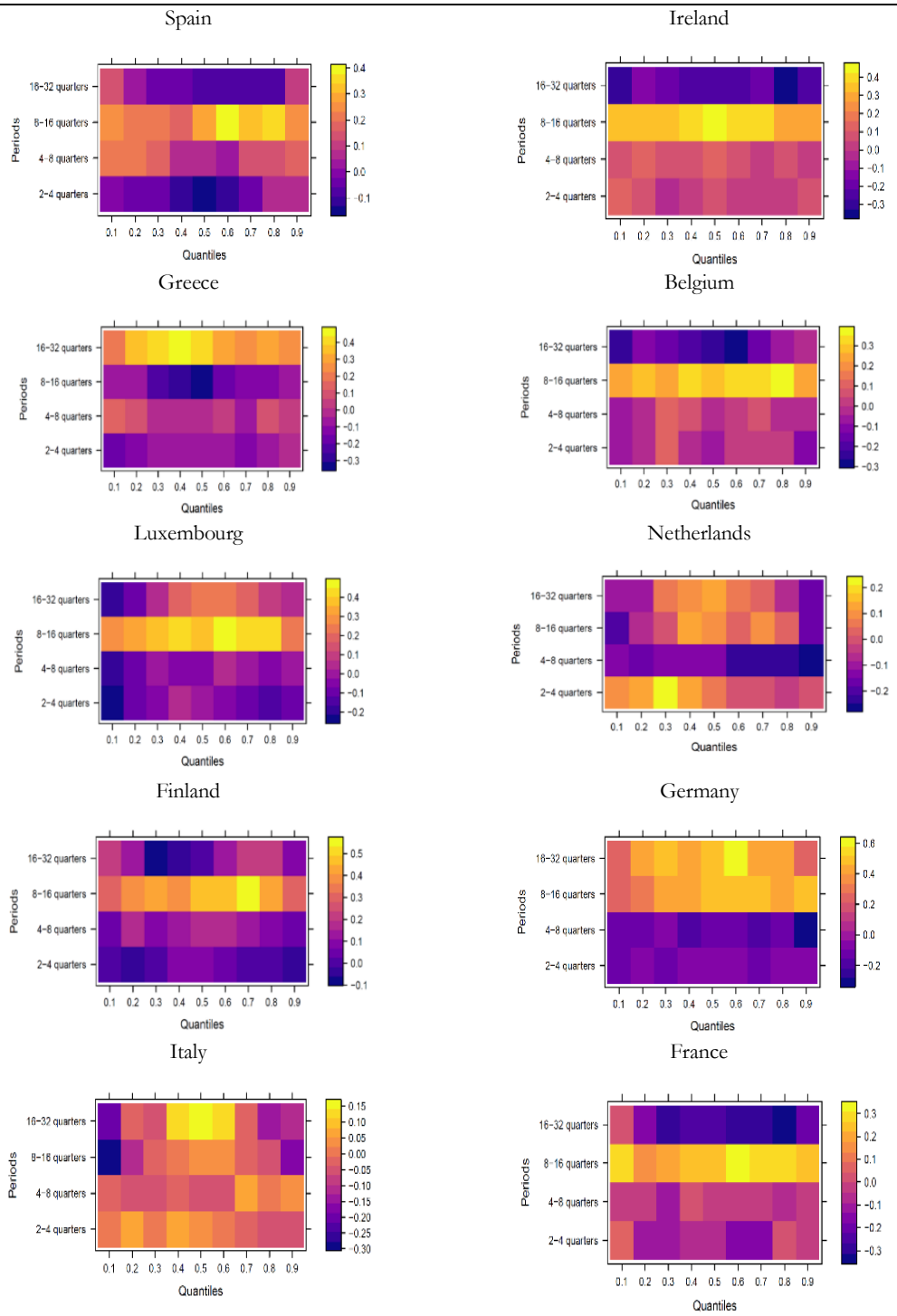

Source: Authors.

Overall, our results stress the importance of working within a nonlinear approach to study the relationship between Δq and Δtb. Since the literature has widely recognized that macroeconomic variables and processes have nonlinear structures, the information obtained from linear models might not be enough to reliably forecast. Shin et al. (2014) warn that the assumption of linear adjustments may be too restrictive in many economically interesting situations, especially where transaction costs are important and where policy interventions

are observed in-sample. In our case, the adjustment process has proven to be nonlinear for some countries.

5. Conclusions

This paper has used time and frequency-domain causality tests to analyze if depreciations (appreciations) of the real effective exchange rate based on unit labor costs led to improvements (deteriorations) in the trade balance in Spain, Ireland, Italy, Greece, Belgium, Luxemburg, Netherlands, Germany, France, and Finland, during 1995-2019.

The time-domain tests used in this paper have several benefits: (i) they are robust to parameter instability/structural breaks; (ii) they consider nonlinear effects and discriminates between negative and positive shocks; and (iii) they allow eliminating the variations related to the seasonal pattern present in macroeconomic series. Within the time-domain approach, we have found no evidence of a clear pattern of causality from depreciations (appreciations) to improvements (deteriorations) in the trade balance improvements.

We have also tested causality between exchange rate and trade balance using frequency-domain approaches. These allow for non-linearities and causality cycles, i.e., causality at high, intermediate, or low frequencies, thereby differentiating between causality in the short, medium, and long run. The conclusions obtained using this approach are generally not different from those in the time domain: there is not any robust evidence of a causal relationship from changes in exchange rates to changes in the trade balances.

Our results indicate that trade imbalances among Euro countries might have not been corrected as a result of changes of the exchange rate. In line with Bajo-Rubio et al. (2016), Xifré (2017), and Bilbao-Ubillos and Fernández-Sainz (2019, 2022), our results suggest that, overall, the trade balances of the Euro Zone economies do not depend much on prices and costs. This means that other factors, such as the increasing participation of countries in global value chains, market accessibility, market size, Ricardian technological advantage, and the institutional and political framework, are possibly more determinant. These will be the subject of future research.

Appendix: Causality Tests implemented

A series x_t is said to Granger-cause another variable y_t if past values of $\mathrm{x_t}$ help forecast future values of y_t beyond the information provided by past values of y_t. We test the null hypothesis of Granger-noncausality from Δq_t to Δtb_t as:

$$H_0^{\Delta q \nrightarrow \Delta tb}: F_{\Delta tb}\left(\Delta tb \middle| I_t^{\Delta tb}, I_t^{\Delta q}\right) = F_{\Delta tb}\left(\Delta tb \middle| I_t^{\Delta tb}\right), \text{ for all } \Delta tb \in \mathbb{R}, \tag{A1}$$

where $I_t \equiv (I_t^{\Delta tb}, I_t^{\Delta q})' \in \mathbb{R}^d$, where $\mathrm{I_t^{\Delta tb}}$ and $\mathrm{I_t^{\Delta q}}$ denote the past information sets of $\mathrm{\Delta tb_t}$ and $\mathrm{\Delta q_t}$, and $\mathrm{F_{\Delta tb}\left(\cdot \middle| I_t^{\Delta tb}, I_t^{\Delta q}\right)}$ is the conditional distribution function of $\mathrm{\Delta tb_t}$ given $(\mathrm{I_t^{\Delta tb}}, \mathrm{I_t^{\Delta q}})$.

A. Time Domain Tests

(i) Troster (2018)

Let assume that $\mathrm{Q_\tau^{\Delta tb,\Delta q}\left(\cdot \middle| I_t^{\Delta tb}, I_t^{\Delta q}\right)}$ denotes the τ-quantile of $\mathrm{F_{\Delta tb}\left(\cdot \middle| I_t^{\Delta tb}, I_t^{\Delta q}\right)}$. Then, the null hypothesis of no Granger causality is:

$$H_0^{QC:\Delta q \nrightarrow \Delta tb}: Q_\tau^{\Delta tb,\Delta q}\left(\Delta tb_t \middle| I_t^{\Delta tb}, I_t^{\Delta q}\right) = Q_\tau^{\Delta tb}\left(\Delta tb_t \middle| I_t^{\Delta tb}\right), \text{ for all } \tau \in \mathcal{T}. \tag{A2}$$

We then use three quantile auto-regressive (QAR) models $\mathrm{m(\cdot)}$, for all $\mathrm{\tau \in \mathcal{T} \subset [0,1]}$:

$$QAR(1): m^1\left(I_t^{\Delta tb}, \theta(\tau)\right) = \mu_1(\tau) + \mu_2(\tau)\Delta tb_{t-1} + \sigma_t \Phi_u^{-1}(\tau) \tag{A3}$$

$$QAR(2): m^2\left(I_t^{\Delta tb}, \theta(\tau)\right) = \mu_1(\tau) + \mu_2(\tau)\Delta tb_{t-1} + \mu_3(\tau)\Delta tb_{t-2} + \sigma_t \Phi_u^{-1}(\tau) \tag{A4}$$

$$\begin{gathered} QAR(3): m^3\left(I_t^{\Delta tb}, \theta(\tau)\right) \\ = \mu_1(\tau) + \mu_2(\tau)\Delta tb_{t-1} + \mu_3(\tau)\Delta tb_{t-2} + \mu_4(\tau)\Delta tb_{t-3} + \\ \sigma_t \Phi_u^{-1}(\tau), \end{gathered} \tag{A5}$$

where the parameters $\theta(\tau) = (\mu_1(\tau), \mu_2(\tau), \mu_3(\tau), \mu_4(\tau), \sigma_t)'$ are estimated with maximum likelihood in an equally-spaced grid of quantiles. $\Phi_u^{-1}(\cdot)$ is the inverse of a standard normal distribution function, while the estimation of the quantile autoregressive models in equation (8) indicates the sign of the causal relationship among the variables.

(ii) Balcilar et al. (2017)

According to Jeong et al. (2012), the variable Δq_t does not Granger-cause the variable Δtb_t in the τ-th quantile if:

$$Q_\tau\{\Delta tb_t|\Delta tb_{t-1},\dots,\Delta tb_{t-p};\ \Delta q_{t-1},\dots,\Delta q_{t-p}\} = Q_\tau\{\Delta tb_t|\Delta tb_{t-1},\dots\Delta tb_{t-p}\}, \quad \text{(A6)}$$

while Δq_t Granger-causes Δtb_t in the τ-th quantile if:

$$Q_\tau\{\Delta tb_t|\Delta tb_{t-1},\dots,\Delta tb_{t-p};\ \Delta q_{t-1},\dots,\Delta q_{t-p}\} \neq Q_\tau\{\Delta tb_t|\Delta tb_{t-1},\dots\Delta tb_{t-p}\}, \quad \text{(A7)}$$

where $\mathrm{Q}_\tau\{\Delta \mathrm{tb}_\mathrm{t}|\cdot\}$ is the τ-th quantile of $\Delta \mathrm{tb}_\mathrm{t}$. If $TB_{t-1} \equiv (\Delta tb_{t-1},\dots,\Delta tb_{t-p}), W_{t-1} \equiv (\Delta tb_{t-1},\dots,\Delta tb_{t-p},\Delta q_{t-1},\dots,\Delta q_{t-p})$, and $V_t = (TB_t, W_t)$, then $F_{\Delta tb_t|W_{t-1}}(\Delta tb_t, W_{t-1})$ and $F_{\Delta tb_t|TB_{t-1}}(\Delta tb_t, TB_{t-1})$ are the conditional distribution functions of $\Delta \mathrm{tb}_\mathrm{t}$ given $\mathrm{TB}_{\mathrm{t}-1}$ and $\mathrm{W}_{\mathrm{t}-1}$, respectively. Jeong et al. (2012) assume that $F_{\Delta tb_t|W_{t-1}}(\Delta tb_t, W_{t-1})$ is absolutely continuous in Δtb_t for almost all V_{t-1}. If we denote $Q_\tau(W_{t-1}) \equiv Q_\tau(\Delta tb_t|W_{t-1})$ and $Q_\tau(TB_{t-1}) \equiv Q_\tau(\Delta tb_t|TB_{t-1})$, then the null hypothesis of no Granger causality from Δq_t to Δtb_t in the τ-th quantile is:

$$H_0 = P\{F_{\Delta tb_t|W_{t-1}}\{Q_\tau(TB_{t-1})|W_{t-1}\} = \tau\} = 1, \quad \text{(A8)}$$

while the hypothesis that Δq_t Granger-causes Δtb_t in the τ-th quantile is:

$$H_1 = P\{F_{\Delta tb_t|W_{t-1}}\{Q_\tau(TB_{t-1})|W_{t-1}\} = \tau\} < 1. \quad \text{(A9)}$$

Jeong et al. (2012) use the distance measure $J = \{\varepsilon_\mathrm{t}\mathrm{E}(\varepsilon_\mathrm{t}|\mathrm{W}_{\mathrm{t}-1})f_\mathrm{W}(\mathrm{W}_{\mathrm{t}-1})\}$, where ε_t and $f_\mathrm{W}(\mathrm{W}_{\mathrm{t}-1})$ are the regression error term and the marginal density function of W_{t-1}, respectively. Since ε_t is true only if $E[1\{\Delta tb_t \leq Q_\tau(TB_{t-1})|W_{t-1}\}] = 0$, Jeong et al. (2012) specify the distance function as:

$$J = E\left[\{F_{\Delta tb_t|W_{t-1}}\{Q_\tau(TB_{t-1})|W_{t-1}\} - \tau\}^2 f_W(W_{t-1})\right]. \quad \text{(A10)}$$

In Equation (A10), $J \geq 0$ if H_0 holds, while $J < 0$ if H_1 holds. Jeong et al. (2012) show that a feasible kernel-based test statistic for J is as follows:

$$\hat{J}_T = \frac{1}{T(1-1)h^{2p}} \sum_{t=k+1}^{T} \sum_{s=k+1, s\neq t}^{T} K\left(\frac{W_{t-1}-W_s}{h}\right) \hat{\varepsilon}_t \hat{\varepsilon}_s, \quad \text{(A11)}$$

where $\mathrm{K}(\cdot)$ denotes the kernel function with bandwidth h and T, k, $\hat{\varepsilon}_\mathrm{t}$ are the sample size, the lag-order and estimate of the unknown regression error, respectively. The estimate of the regression error is the following:

$$\hat{\varepsilon}_t = 1\{\Delta tb_t \leq Q_\tau(TB_{t-1}) - \tau\}. \quad \text{(A12)}$$

We further use the nonparametric kernel method to estimate the τ-th conditional quantile of Δtb_t given TB_{t-1} as $\hat{Q}_\tau(TB_{t-1}) = \hat{F}^{-1}_{\Delta tb_t|TB_{t-1}}(\tau|TB_{t-1})$, where $\hat{F}_{\Delta tb_t|TB_{t-1}}(\Delta tb_t|TB_{t-1})$ is the Nadarya-Watson kernel estimator:

$$\hat{F}_{\Delta tb_t|TB_{t-1}}(\Delta tb_t|TB_{t-1}) = \frac{\sum_{s\neq t} L\left((TB_{t-1} - TB)/h\right)1(TB_s \leq TB_{t-1})}{\sum_{s\neq t} L\left((TB_{t-1} - TB)/h\right)} \quad \text{(A13)}$$

where with $\mathrm{L}(\cdot)$ denotes the kernel function and h is the bandwidth.

Balcilar et al. (2017) extend the framework of Jeong et al. (2012) by developing a test for the second moment, thereby adopting the nonparametric Granger-quantile-causality approach by Nishiyama et al. (2011). With the inclusion of the Jeong et al. (2012) approach, Balcilar et al. (2017) overcome the issue that causality in mean implies causality in variance, thus the hypothesis of quantile Granger causality running from Δq_t to Δtb_t in higher-order moments can be specified as:

$$H_0 = P\left\{F_{\Delta tb_t^K|W_{t-1}}\{Q_\tau(TB_{t-1})|W_{t-1}\} = \tau\right\} = 1 \; for \; k = 1, 2, \ldots, K, \quad \text{(A14)}$$

and

$$H_1 = P\left\{F_{\Delta tb_t^K|W_{t-1}}\{Q_\tau(TB_{t-1})|W_{t-1}\} = \tau\right\} < 1 \; for \; k = 1, 2, \ldots, K. \quad \text{(A15)}$$

Jeong et al. (2012) show that the re-scaled statistics $Th^p\hat{J}_T/\hat{\sigma}_0$ is asymptotically normally distributed. To begin with, we test for the nonparametric granger causality in mean (k=1). Failure to reject the null of Granger causality in mean does not imply non-causality in variance. Therefore, we construct the tests for k=2. The last step is to test for causality-in-mean and variance successively. We determine the lag order using SIC of Schwarz (1978). The bandwidth is selected through the use of least squares cross-validation method. We use the Gaussian kernels for $\mathrm{K}(\cdot)$ and $\mathrm{L}(\cdot)$.

(iii) Hacker and Hatemi-J (2012)

The test departs from the lag-augmented VAR (LA-VAR) model specification of Toda and Yamamoto (2000) and the relevant causality test is:

$$Y = DZ + \delta. \quad \text{(A16)}$$

where $Y := (y_1, y_2, \ldots, y_T)$ is an $(n \times T)$ matrix in which n is the number of variables and T is the sample size. In this framework, $D := (\alpha, A_1, A_2, \ldots, A_k)$ is an $(n \times (1 + (k + d_{\max}))$ matrix and $Z := (Z_0, Z_1, \ldots, Z_{T-1})$ denotes a $((1 + n(k + d_{\max})) \times T)$ matrix. Thus, a matrix can be written as:

$$Z_t := \begin{bmatrix} 1 \\ y_t \\ y_{t-1} \\ \cdot \\ \cdot \\ y_{t-k+1} \end{bmatrix}$$

and $\delta := (u_1, u_2, \ldots, u_T)$ represents a $(n \times T)$ matrix. Equation (A16) constitutes a framework test for the null of no causality. The null hypothesis of Granger-noncausality is:

$$H_0: C\beta = 0 \tag{A17}$$

which can be tested through the following Wald statistic:

$$\text{Wald} = (C\beta)'[C((Z'Z)^{-1} \otimes S_u)C']^{-1}(C\beta) \sim X_p^2 \tag{A18}$$

where $\beta = vec(D)$, vec is the column-stacking operator, $\otimes$ is the Kronecker product, C is a (p × n)(1 + p × n) indicator matrix with ones and zeros, and S_u is the variance-covariance matrix of the unrestricted VAR model. Under the conditional of normal distribution, the Wald statistic in Equation (A18) has a $\chi 2$ distribution asymptotically with p degrees of freedom. However, if the sample size is small and the assumption of normality is violated with time-varying volatility, then the asymptotic critical values for the Wald test are not precise. To deal with it, we will apply the bootstrap test with leverage adjustment as suggested by Hacker and Hatemi-J (2012). This test allows for the role of time-varying effects performs also well when the lag order is endogenously selected. In this context, we first computed the sub-sample size (ss) within equation (A19) to implement the time-varying form of the Hacker and Hatemi-J (2012) causality test.

$$ss = \left[T\left(0.01 + 1.8/\sqrt{T}\right)\right] \tag{A19}$$

Equations (A16)-(A19) consider the role of time-varying effects, while we enhanced the empirical analysis by incorporating asymmetry. To this aim, we assess the relationships between q_t and tb_t departing from the linear regression model, defined as $tb_t = \delta_0 + \delta_1 q_t + \psi D_t + \omega_t$. Additionally, we consider the role of asymmetry: Let us assume that q_t is an integrated variable with data generating process $q_t \equiv q_{t-1} + e_{1t} = q_0 + \sum_{i=1}^{T} e_{1i}$, where q_0 is the initial value of q, and $\mathrm{e_{1i}}$ is i.i.d. with variance $\sigma_{e_1}^2$. In Hatemi-J (2012), positive shocks are defined as $e_{1t}^+ = max(e_{1t}, 0)$; while negative shocks are defined as $e_{1t}^- = min(e_{1t}, 0)$. This implies that $e_{1t} = e_{1t}^+ + e_{1t}^-$; while $q_t = q_0 + \sum_{i=1}^{t} e_{1t}^+ + \sum_{i=1}^{t} e_{1t}^-$. Hatemi-J (2012) defines positive and negative shocks of each variable in a cumulative form as $q_t^+ = \sum_{i=1}^{t} e_{1t}^+$ and $q_t^- = \sum_{i=1}^{t} e_{1i}^-$.

B. Combined Time- and frequency-domain causality tests

(iv) Partial Wavelet Coherence

The wavelet partial spectrum (WPS), denoted $[W_n^x]^2$, assesses the local variance of each variable. By means of Monte Carlo simulations, Torrence and Compo (1998) show that the distribution of the local WPS can be expressed as:

$$D\left(\frac{[W_n^x(s)]^2}{\sigma_x^2} < p\right) \rightarrow \frac{1}{2} P_f x_v^2. \tag{A20}$$

The Cross-Wavelet Power (CWP) indicates the zone in the time-scale domain where the time series display high mutual power. The CWP captures the local covariance of two time series in each frequency and shows the quantitative similarities between them. This allows us to locate the regions where Δq_t and Δtb_t co-move in the time-frequency space. For each signal Δq and Δtb we specify the individual wavelet spectra as $W_n^{\Delta q}(s)$ and $W_n^{\Delta tb}(s)$. The Cross-Wavelet between two signals is expressed as:

$$CWS_n^{\Delta q \Delta tb}(s) = W_n^{\Delta q}(s) W_n^{\Delta tb^*}(s), \tag{A21}$$

where $W_n^{\Delta tb^*}$ is the complex conjugate of $W_n^{\Delta tb}(s)$. The CWP is thus defined as $\left|W_n^{\Delta q \Delta tb}\right|$

The Wavelet Coherence (WC) of two series $\Delta q = \{\Delta q_n\}$ and $\Delta tb = \{\Delta tb_n\}$ is the localized correlation coefficient among these variables in the time-frequency domain. We calculate the WC as the squared absolute value of the smoothed CWS normalized by the product of the smoothed individual WPS of each variable:

$$R^2(u,s) = \frac{\left|S\left(s^{-1} W_{\Delta q \Delta tb}(u,s)\right)\right|^2}{S\left(s^{-1}\left|W_{\Delta q}(u,s)\right|^2\right) S(s^{-1}|W_{\Delta tb}(u,s)|^2)} \tag{A22}$$

(v) Wavelet Quantile Correlation

Following Li et al. (2015), $Q_{\tau,\Delta q}$ is the τ-th quantile of Δq, and $Q_{\tau,\Delta tb}(\Delta q)$ the τ-th quantile of Δtb conditioning on Δq. Δq is assumed to be independent of Δtb. The quantile covariance can be explained as:

$$\begin{aligned} Qcov_t(\Delta tb, \Delta q) &= cov\{I(\Delta tb - Q_{\tau,Y} > 0, \Delta q)\} \\ &= E(\varphi_\tau(\Delta tb - Q_{\tau,Y})(\Delta q - E(Y)), \end{aligned} \tag{A23}$$

where $0 < \tau < 1$ and $\varphi_\tau(w) = \tau - I(w < 0)$. Following Li et al. (2015 we calculate the quantile correlation as:

$$QC_t(\Delta tb, \Delta q) = \frac{cov_t(\Delta tb, \Delta q)}{\sqrt{var(\varphi_\tau(\Delta tb - Q_{\tau,\Delta tb}))var(\Delta q)}} \tag{A24}$$

The quantile correlation method is extended by Kumar and Padakandla (2022) by means of a maximal overlapping discrete wavelet transform for decomposing Δq_t and Δtb_t. Pairs of Δq_t and Δtb_t are decomposed at the j_{th} level, and quantile correlation techniques are applied to get the wavelet quantile correlation for each level j. Wavelet quantile correlation is:

$$WQC_t(\Delta tb, \Delta q) = \frac{QC_t(d_j[\Delta tb], d_j[\Delta q])}{\sqrt{var(\theta_\tau(d_j[\Delta tb] - Q_{\tau, d_j[\Delta tb]}))var(d_j[\Delta q])}} \quad \text{(A25)}$$

In Equation (A25), Δq is the independent series and Δtb the dependent series. By representing the association between Δq and Δtb at different quantiles, wavelet quantile correlation handles the effects of the outliers as shocks and captures the likely asymmetric associations between the model parameters.

References

Ahmed, A., Granberg, M., Troster, V., & Uddin, G. S. (2022). Asymmetric dynamics between uncertainty and unemployment flows in the United States. *Studies in Nonlinear Dynamics and Econometrics*, *26*(1), 155–172. https://doi.org/10.1515/SNDE-2019-0058/DOWNLOADASSET/SUPPL/J_SNDE-2019-0058_SUPPL.ZIP

Allsop, C., & Vines, D. (2010). Fiscal Policy, intercountry adjustment and the real exchange rate within Europe. In M. Buti et al. (Ed.), *The Euro: The First Decade*. Cambridge University Press. https://ideas.repec.org/p/euf/ecopap/0344.html

Bahmani, M., Harvey, H., & Hegerty, S. W. (2013). Empirical tests of the Marshall-Lerner condition: A literature review. *Journal of Economic Studies*, *40*(3), 411–443. https://doi.org/10.1108/01443581311283989/FULL/PDF

Bahmani-Oskooee, M., & Nouira, R. (2021a). U.S.-German commodity trade and the J-curve: New evidence from asymmetry analysis. *Economic Systems*, *45*(2), 100779. https://doi.org/10.1016/J.ECOSYS.2020.100779

Bahmani-Oskooee, M., & Nouira, R. (2021b). U.S. – Italy commodity trade and the J-curve: new evidence from asymmetry analysis. *International Economics and Economic Policy*, *18*(1), 73–103. https://doi.org/10.1007/S10368-020-00472-4/FIGURES/1

Bajo-Rubio, O., Berke, B., & Esteve, V. (2016). The effects of competitiveness on trade balance: The case of southern europe. *Economics*, *10*(1), 1–26.

Balcilar, M., Bekiros, S., & Gupta, R. (2017). The role of news-based uncertainty indices in predicting oil markets: a hybrid nonparametric quantile causality method. *Empirical Economics*, *53*(3), 879–889. https://doi.org/10.1007/S00181-016-1150-0/FIGURES/2

Belke, A., & Dreger, C. (2013). Current Account Imbalances in the Euro Area: Does Catching up Explain the Development? *Review of International Economics*, *21*(1), 6–17. https://doi.org/10.1111/ROIE.12016

Bilbao-Ubillos, J., & Fernández-Sainz, A. (2019). A critical approach to wage devaluation: The case of Spanish economic recovery. *The Social Science Journal*, *56*(1), 88–93. https://doi.org/10.1016/J.SOSCIJ.2018.05.006

Bilbao-Ubillos, J., & Fernández-Sainz, A.-I. (2022). The results of internal devaluation policy as a crisis exit strategy: The case of Spain. *Global Policy*. https://doi.org/10.1111/1758-5899.13120

Brock, W. A., Scheinkman, J. A., Dechert, W. D., & LeBaron, B. (1996). A test for independence based on the correlation dimension. *Econometric Reviews*, *15*(3), 197–235. https://doi.org/10.1080/07474939608800353

El-Shagi, M., Lindner, A., & von Schweinitz, G. (2016). Real Effective Exchange Rate Misalignment in the Euro Area: A Counterfactual Analysis. *Review of International Economics*, *24*(1), 37–66. https://doi.org/10.1111/ROIE.12207

European Commission. (2011). *Quarterly Report on the Euro Area*. Office for Official Publ. of the European Communities.

Fukui, M., Nakamura, E., & Steinsson, J. (2023). *The Macroeconomic Consequences of Exchange Rate Depreciations* (w31279).

Goldstein, M., & Khan, M. S. (1985). Income and price effects in foreign trade. *Handbook of International Economics*, *2*(C), 1041–1105. https://doi.org/10.1016/S1573-4404(85)02011-1

Granger, C. W. J. (1969). Investigating Causal Relations by Econometric Models and Cross-spectral Methods. *Econometrica*, *37*(3), 424. https://doi.org/10.2307/1912791

Hacker, S., & Hatemi-J, A. (2012). A bootstrap test for causality with endogenous lag length choice: Theory and application in finance. *Journal of Economic Studies*, *39*(2), 144–160. https://doi.org/10.1108/01443581211222635/FULL/PDF

Hatemi-J, A. (2012). Asymmetric causality tests with an application. *Empirical Economics*, *43*(1), 447–456. https://doi.org/10.1007/S00181-011-0484-X

Jeong, K., Härdle, W. K., & Song, S. (2012). A consistent nonparametric test for causality in quantile. *Econometric Theory*, *28*(4), 861–887. https://doi.org/10.1017/S0266466611000685

Kilian, L. (2019). Measuring global real economic activity: Do recent critiques hold up to scrutiny? *Economics Letters*, *178*, 106–110. https://doi.org/10.1016/J.ECONLET.2019.03.001

Krugman, P. (2012). *End This Depression Now!* WW Norton & Company.

Krugman, P., & Taylor, L. (1978). Contractionary effects of devaluation. *Journal of International Economics*, *8*(3), 445–456. https://doi.org/10.1016/0022-1996(78)90007-7

Kumar, A. S., & Padakandla, S. R. (2022). Testing the safe-haven properties of gold and bitcoin in the backdrop of COVID-19: A wavelet quantile correlation approach. *Finance Research Letters*, *47*, 102707. https://doi.org/10.1016/J.FRL.2022.102707

Li, G., Li, Y., & Tsai, C. L. (2015). Quantile Correlations and Quantile Autoregressive Modeling. *Journal of the American Statistical Association*, *110*(509), 246–261. https://doi.org/10.1080/01621459.2014.892007

Magee, S. P. (1973). Currency Contracts, Pass-Through, and Devaluation. *Brookings Papers on Economic Activity*, *1973*(1), 325. https://doi.org/10.2307/2534091

Mazzocchi, R., & Tamborini, R. (2021). Current account imbalances and the Euro Area. Controversies and policy lessons. *Economia Politica*, *38*(1), 203–234. https://doi.org/10.1007/S40888-021-00214-Y/FIGURES/10

Nishiyama, Y., Hitomi, K., Kawasaki, Y., & Jeong, K. (2011). A consistent nonparametric test for nonlinear causality—Specification in time series regression - ScienceDirect. *Journal of Econometrics*, *165*(1), 112–127. https://www.sciencedirect.com/science/article/pii/S0304407611001023

Nogueira, R. P., & León-Ledesma, M. A. (2011). Does Exchange Rate Pass-through Respond TO Measures Of Macroeconomic Instability? *Journal of Applied Economics*, *14*(1), 167–180. https://doi.org/10.1016/S1514-0326(11)60010-X

Percival, D., & Walden, A. (2000). *Wavelet methods for time series analysis*. Cambridge University Press.

Rose, A. K., & Yellen, J. L. (1989). Is there a J-curve? *Journal of Monetary Economics*, *24*(1), 53–68. https://doi.org/10.1016/0304-3932(89)90016-0

Schwarz, G. (1978). Estimating the Dimension of a Model. *The Annals of Statistics*, *6*(2), 461–464. https://doi.org/10.1214/aos/1176344136

Shin, Y., Yu, B., & Greenwood-Nimmo, M. (2014). Modelling Asymmetric Cointegration and Dynamic Multipliers in a Nonlinear ARDL Framework. In *Festschrift in Honor of Peter Schmidt* (pp. 281–314). Springer New York. https://doi.org/10.1007/978-1-4899-8008-3_9

Toda, H. Y., & Yamamoto, T. (1995). Statistical inference in vector autoregressions with possibly integrated processes. Journal of Econometrics, 66(1–2), 225–250. https://doi.org/10.1016/0304-4076(94)01616-8

Torrence, C., & Compo, G. P. (1998). A Practical Guide to Wavelet Analysis. *Bulletin of the American Meteorological Society*, *79*(1), 61–78. https://doi.org/10.1175/1520-0477(1998)079

Troster, V. (2018). Testing for Granger-causality in quantiles. *Econometric Reviews*, *37*(8), 850–866. https://doi.org/10.1080/07474938.2016.1172400

Xifré, R. (2017). Competitividad y comportamiento de las exportaciones: España en el contexto de la eurozona. *Cuadernos de Información Económica*, *260*, 27–37. http://ec.europa.eu/economy_finance/db_indicators/competitiveness/

Yilanci, V., & Kilci, E. N. (2021). The role of economic policy uncertainty and geopolitical risk in predicting prices of precious metals: Evidence from a time-varying bootstrap causality test. *Resources Policy*, *72*, 102039. https://doi.org/10.1016/J.RESOURPOL.2021.102039